ASIAN JOURNAL OF CIVIL ENGINEERING (BUILDING AND HOUSING) VOL. 11, NO. 3 (2010)
PAGES 295-319

MODELING PROBABILISTIC CRITICAL EARTHQUAKE INPUTS FOR STRUCTURES USING THE SITE RESPONSE SPECTRA

A. Moustafa[*a] and S. Mahadevan[b]
[a]Department of Civil Engineering, Minia University, Minia 61111, Egypt
[b]Department of Civil and Environmental Engineering, Vanderbilt University, Nashville, TN 37235, USA

ABSTRACT

This paper develops a reliability-based computational methodology for modeling non-stationary random critical earthquake loads on structures using the site response spectra. The power spectral density function and the envelope parameters of the ground acceleration are taken to be unknown and are computed such that the structural reliability index is minimized subjected to constraints reflecting known knowledge on the site seismicity. Specifically, bounds on the total energy, zero-crossing rate and entropy rate of the earthquake signal and positivity requirements are considered. These constraints are derived from the site response spectra. The formulation combines methods of structural reliability analysis, response surface fitting, FORM and nonlinear programming. Numerical illustrations on reliability-based critical earthquake inputs for elastic and inelastic frame structures are presented.

Keywords: Critical earthquake; random processes; structural reliability; FORM, response surface; nonlinear optimization

1. INTRODUCTION

Earthquake ground motions exhibit large variability in terms of their frequency of occurrence, time, location, and several other parameters such as magnitude, intensity, duration, peak values of ground acceleration, velocity and displacement, frequency content and amplitude. In some situations, the available seismic data is scarce, inhomogeneous or insufficient. In this context, the method of critical earthquake load modeling provides a framework to deal with seismic safety assessment of engineering structures under partially specified earthquake loads. Takewaki [1,2], Abbas and Manohar [3] and Abbas [4,5] provide an overview of this method. The unknown information on the input is computed by solving an inverse dynamic problem such that the structure performance is minimized. At the same time, the earthquake load satisfies bounds that reflect known characteristics of

[*] E-mail address of the corresponding author: abbas.moustafa@yahoo.com (A. Moustafa)

recorded ground motions. The resulting earthquake input is termed '*critical*' since it produces the least structural performance and thus provides an idea about the worst case scenario that can happen to the structure.

The method of critical excitations was introduced to earthquake engineering by Drenick [6], Shinozuka [7] and Iyengar [8]. Drenick [9] expressed the future earthquake acceleration as a linear summation of past recorded accelerograms with unknown coefficients. He computed the critical acceleration by maximizing the structure response subjected to a bound on the acceleration energy. Abbas and Manohar [3] represented the ground acceleration as a Fourier series modulated by an enveloping function, thus ensuring convergence and orthogonality in the basis functions. The set of past recorded ground motions were used instead in quantifying the constraints imposed on the earthquake load, and, also, in defining the parameters of the envelope function.

Iyengar and Manohar [10] developed non-stationary random critical earthquake excitations for linear multi-degree-of-freedom (MDOF) structures. The input was constrained to the average total energy and the structure response variance was maximized. Several improvements to this method were introduced by Iyengar [11], Manohar and Sarkar [12], Takewaki [13] and Abbas and Manohar [3]. In most of these studies, the earthquake load is assumed to be a Gaussian random process of zero mean and the structure behavior is considered to be linear. The response process is thus Gaussian and is characterized by its variance (mean is zero). The critical earthquake loads were thus computed by maximizing the response variance. For nonlinear systems, this approach is not applicable since the response of nonlinear systems is non-Gaussian (even if the input is Gaussian) and mean is nonzero. Therefore, critical excitations that maximize the structure response variance are of limited significance. Takewaki [14] modeled critical random earthquake excitations for elastic-plastic structures using equivalent linearization.

The development of reliability-based critical earthquake loads for linear systems was carried out by Abbas [4], Sarkar [15], Saikat and Manohar [16] and Abbas and Manohar [17]. The study by Abbas and Manohar [18] extends the formulation to nonlinear structures with cubic force-displacement relation. The modeling of critical seismic loads for parametrically excited structures was studied by Abbas and Manohar [19].

This paper develops a reliability-based methodology to estimate non-stationary random critical earthquake loads on structures using response spectra. The structural response process in this case has non zero mean and non-stationary variance. To derive critical seismic inputs for this problem one approach is to maximize both the mean and variance of the structural response following previous studies. An alternative approach pursued in this paper is to maximize the failure probability of the structure. This approach is easier to implement than the bi-objective optimization and is also more comprehensive because it accounts for randomness in the structural system parameters. This paper uses the site design response spectrum in quantifying the constraints. The proposed methodology is more practical since it is easier to find a response spectrum for the site rather than detailed information on past recorded ground motions. Furthermore, the study accounts for uncertainties in the PSD and the envelope functions of the earthquake load by treating these parameters as unknowns. Numerical examples on modeling reliability-based random non-stationary critical earthquake loads on elastic and inelastic frame structures are provided.

2. RELIABILITY-BASED CRITICAL EARTHQUAKE LOADS FOR ELASTIC STRUCTURES USING THE SITE RESPONSE SPECTRA

2.1 Dynamic analysis of elastic MDOF structures under earthquake loads

The equation that governs the relative displacement response **u***(t)* for an elastic *N* degree-of-freedom system is given by:

$$\mathbf{M}\,\ddot{\mathbf{u}}(t) + \mathbf{C}\,\dot{\mathbf{u}}(t) + \mathbf{K}\,\mathbf{u}(t) = -\mathbf{M}\,\{\mathbf{1}\}\,\ddot{u}_{\mathrm{g}}(t). \tag{1}$$

Here, **M**, **C**, **K** are, respectively, the mass, damping and stiffness matrices of the discretized *N* degree-of-freedom structure, **{1}** is a column vector of ones and $\ddot{u}_{\mathrm{g}}(t)$ is a stochastic process representing the earthquake acceleration. Assuming that the system starts from rest, damping to be proportional, and expressing the displacement response in terms of the superposition of the modal contributions $u(t) = \sum_{n=1}^{\infty} \phi_n q_n(t)$, the above equation of motion reduces to:

$$\ddot{q}(t) + 2\varsigma_n \omega_n \dot{q}(t) + \omega_n^2\, q(t) = -\gamma_n\, \ddot{u}_{\mathrm{g}}(t); \quad \gamma_n = \frac{\phi_{\mathrm{n}}^{\mathrm{T}}\mathbf{M}\{\mathbf{1}\}}{\phi_n^T \mathbf{M} \phi_n}, \tag{2}$$

where, $\varsigma_n, \omega_n, \gamma_n$ are the damping ratio, natural frequency, participation factor for the *n*th mode, respectively and ϕ is the matrix of mode shapes. The *i*th displacement response can be shown to be given by:

$$u_i(t) = \sum_{j=1}^{N} \gamma_j \phi_{ij} \int_0^t \ddot{u}_{\mathrm{g}}(\tau) h_j(t-\tau) d\tau \tag{3}$$

Here, $h_j(t)$ is the *j*th impulse response function. The determination of the displacement response $u_i(t)$ is often carried out by numerical integration of Eq. (3). Additionally, the series representation of the displacement response **u**(*t*) needs to be truncated and this will be demonstrated in the numerical example. Referring to Eq. (3) the displacement random process has a zero mean if $\ddot{u}_{\mathrm{g}}(t)$ has a zero mean. Furthermore, the response variance of the *i*th displacement component is given as:

$$\overline{\sigma}_{u_i}^2(t) = \sum_{j=1}^{N}\sum_{k=1}^{N} \gamma_j \gamma_k \phi_{ij} \phi_{kj} \int_0^t \int_0^t < \ddot{u}_{\mathrm{g}}(\tau_1) \ddot{u}_{\mathrm{g}}(\tau_2) > h_j(t-\tau_1) h_k(t-\tau_2) d\tau_1 d\tau_2 \tag{4}$$

Here, <·> denotes the mathematical expectation and the evaluation of the above expression will be demonstrated in the next section.

2.2 Problem statement and solution

Reliability assessment of elastic MDOF structures governed by equations of motion as Eq. (1) or (2) requires the specification of the structure parameters (**M**, **C** and **K**) and the acceleration $\ddot{u}_g(t)$. We assume that the structure parameters are known while only partial information on the earthquake acceleration is available. To proceed further, we model the ground acceleration $\ddot{u}_g(t)$ of Eq. (1) as a non-stationary Gaussian random process given by:

$$\ddot{u}_g(t) = e(t)\ddot{w}_g(t). \tag{5}$$

Here, $e(t)$ is the envelope function that imparts non-stationarity to the ground acceleration and $\ddot{w}_g(t)$ is the stationary acceleration. In the present study, $e(t)$ is expressed as a Gamma model given by:

$$e(t) = \frac{\exp(-\alpha_1 t) - \exp(-\alpha_2 t)}{\max[\exp(-\alpha_1 t) - \exp(-\alpha_2 t)]}; \quad \alpha_2 > \alpha_1 > 0; 0 \le t \le t_d, \tag{6}$$

where α_1, α_2 are the parameters of the envelope function that control the non-stationarity trend of the ground acceleration $\ddot{u}_g(t)$ and t_d is the earthquake duration. The envelope function as per the above definition has a peak value of unity. Furthermore, the acceleration $\ddot{w}_g(t)$ is represented as

$$\ddot{w}_g(t) = \sum_{i=1}^{N_f} [A_i \cos(\omega_i t) + B_i \sin(\omega_i t)], \tag{7}$$

where, A_i, B_i, i = 1,2,…, N_f, are $2N_f$ normal random variables of zero mean and variances σ_i^2 and ω_i, $i = 1,2,..., N_f$ are set of N_f frequencies to be selected to span satisfactory the frequency range (ω_0, ω_c) of the ground acceleration $\ddot{u}_g(t)$. Additionally, the random variables A_i, B_i, i = 1,2,…, N_f are taken to be independent and satisfy the conditions:

$$< A_i A_j > = < B_i B_j > = \sigma_i^2 \delta_{ij}; < A_i B_j > = 0 \; \forall \; i, j = 1,2,.., N_f \tag{8}$$

Here, <·> indicates the mathematical expectation and δ_{ij} is the Kronecker delta function ($\delta_{ij} = 1$; for $i = j$ and $\delta_{ij} = 0$ for $i \neq j$). Under these conditions, the ground acceleration $\ddot{w}_g(t)$ is a stationary Gaussian random process of zero mean. The auto-correlation and the one-sided power spectral density (PSD) functions for $\ddot{w}_g(t)$ can be shown to be given by:

$$R(\tau)=\sum_{i=1}^{N_f}\sigma_i^2\cos(\omega_i\tau);\qquad G(\omega)=\sum_{i=1}^{N_f}\sigma_i^2\delta(\omega-\omega_i);\quad i=1,2,...,N_f \tag{9}$$

According to the representation of the random process $\ddot{w}_g(t)$ in Eq. (7) and from Eqs. (5) and (6), the ground acceleration $\ddot{u}_g(t)$ has zero mean, random amplitude and phase angle of $\sqrt{A_i^{\,2}+B_i^{\,2}}$ and $\theta_i=\tan^{-1}(B_i/A_i)$ at the *i*th frequency, respectively and a peak amplitude of $\sum_{i=1}^{N_f}\sqrt{A_i^2+B_i^2}$. It may be recalled here that the amplitude of the ground acceleration $\ddot{u}_g(t)$ depends on three parameters, namely, the source properties, the path effects and the soil profile effects. From Eq. (4) and the second part of Eq. (9), the structure response variance can be shown to be given as:

$$\begin{aligned}\bar{\sigma}_{u_i}^2(t)&=\int_{\omega_0}^{\omega_c}G(\omega)H_i(\omega,t)d\omega=\sum_{n=1}^{N_f}\sigma_n^2H_i(\omega_n,t);\\ H_i(\omega_n,t)&=\sum_{j=1}^{N}\sum_{k=1}^{N}\gamma_j\gamma_k\varphi_{ij}\varphi_{ik}\int_0^t\int_0^t e(\tau_1)e(\tau_2)h_j(t-\tau_1)h_k(t-\tau_2)\cos\omega_n(\tau_2-\tau_1)d\tau_1d\tau_2\end{aligned} \tag{10}$$

The acceleration $\ddot{w}_g(t)$ is characterized in terms of the PSD function as follows:

$$E_0=\int_{\omega_0}^{\omega_c}G(\omega)d\omega;\quad E_2=\int_{\omega_0}^{\omega_c}\omega^2G(\omega)d\omega \tag{11}$$

The moments E_0 and E_2 represent energy measures for $\ddot{w}_g(t)$. The total energy of the random process $\ddot{u}_g(t)$ is given as:

$$E_T=E_0\int_0^{t_d}e^2(t)\,dt \tag{12}$$

The energy quantities E_0 and E_2 define the zero crossing rate of the earthquake acceleration $\ddot{u}_g(t)$ which is given by:

$$n_0^+=\frac{1}{2\pi}\sqrt{\frac{E_2}{E_0}}. \tag{13}$$

The uncertainty of the random process $\ddot{u}_g(t)$ can be characterized by the entropy rate of

the PSD function $G(\omega)$ as follows [20]:

$$H_{\mathrm{W}} = \log_e \sqrt{2\pi e} + \frac{1}{2(\omega_{\mathrm{c}} - \omega_0)} \int_{\omega_0}^{\omega_{\mathrm{c}}} \log_e [G(\omega)] d\omega. \tag{14}$$

The use of entropy rate in quantifying uncertainty of stochastic processes is well established in the literature, see for example the book by Kapur [21]. Here, it may be noted that, for a given frequency range ($\omega_0, \omega_{\mathrm{c}}$), and for a given total average power, it can be shown that a band limited white noise would possess the highest entropy rate, and, conversely, a narrow band signal would possess the least entropy rate [22]. A realistic ground motion, however, is unlikely to be an ideal band limited white noise or an ideal narrow band signal. The entropy rate associated with realistic ground motion is expected to be bounded between that of an ideal band limited white noise and of an ideal narrow banded signal. Thus, realistic models for critical seismic inputs can be obtained by requiring that these inputs possess entropy rates that are actually observed in recorded ground motions. Manohar and Sarkar [12] and Abbas and Manohar [3] have used the entropy rate as a constraint on the critical earthquake signal. These authors showed that the inclusion of the entropy rate in deriving critical earthquake acceleration is crucial in producing realistic seismic excitations. The development of critical earthquake loads for elastic structures based on the response spectrum is provided in the next section.

2.3 Estimation of critical earthquake excitations using site response spectrum

To assess the reliability of MDOF systems governed by equations of motion such as Eq. (1) we first introduce a performance function as follows [23]:

$$g(R,S) = R - S, \tag{15}$$

where R is the resistance (capacity) of the structure at a certain point and S is the demand (load effect), both corresponding to some response quantity (e.g. displacement, stress, etc.) due to the seismic load. $g(R,S) < 0$ defines the unsafe region, $g(R,S) > 0$ defines the safe region and $g(R,S) = 0$ represents the limit state surface that separates safe and unsafe zones. Since the earthquake load is a function of time, the structural response is also a time-dependent quantity and thus Eq. (15) can be rewritten as:

$$g(R, S\{x_0, t, \ddot{u}_{\mathrm{g}}(t)\}) = R - \max_{0<t<\infty} | z(x_0, t, \alpha_1, \alpha_2, A_1, A_2, ..., A_{N_{\mathrm{f}}}, B_1, B_2, ..., B_{N_{\mathrm{f}}}) | \tag{16}$$

Here, $S(x_0, t, \ddot{u}_{\mathrm{g}}(t))$ is the response or a transformation of it at point x_0 and time t.

The probability of failure $P_f = P[g(\mathbf{X}) < 0]$ and $\mathbf{X} = [R, A_1, A_2, ..., A_{N_{\mathrm{f}}}, B_1, B_2, ..., B_{N_{\mathrm{f}}}]^t$ is the set of basic random variables including the structural resistance R and excitation parameters A_i, B_i. The envelope parameters α_1, α_2 are treated as unknown deterministic variables in the present study. The performance function defined above is an implicit

nonlinear function of the vector of random variables **X**. Approximation for the distribution of the second quantity on the right side of Eq. (16) is limited to simple cases (e.g. linear structural behavior and stationary Gaussian inputs). For more general problems, approximate numerical methods, such as, Monte Carlo simulation (MCS) or response surface methods can be employed in evaluating the structure reliability. In the present study, we restrict to the latter alternative since MCS requires more computational time. Specifically, we adopt the response surface method as developed by Bucher and Bourgund [24]. The implicit performance function of Eq. (16) is replaced by an explicit quadratic surface near the design point. The shortest distance from the origin to this surface provides a measure of the structural reliability in terms of the Hasofer-Lind reliability index. The details of the response surface method are provided in the next section.

The problem of deriving the optimal earthquake loads for elastic structures can be stated as computing the optimal PSD function $G(\omega)$ and the envelope parameters α_1, α_2 such that the structure reliability index is minimized subjected to constraints as follows:

$$\begin{aligned}&\text{Minimize } \beta\\ &\text{Such that } \int_{\omega_0}^{\omega_c} G(\omega)d\omega = \overline{E}_0; \frac{1}{2\pi}\sqrt{\frac{E_2}{E_0}} = \overline{n}_0^+; \frac{1}{2(\omega_c-\omega_0)}\int_{\omega_0}^{\omega_c}\log_e(1+\frac{G(\omega)}{G_0})d\omega \geq \Delta\overline{H}_W \qquad (17)\\ &\alpha_{1l} \leq \alpha_1 \leq \alpha_{1u}; \alpha_{2l} \leq \alpha_2 \leq \alpha_{2u}; \alpha_2 > \alpha_1 > 0.\end{aligned}$$

The constraints listed above include bounds on the average energy, zero crossing rate and amount of disorder of the ground acceleration. The constraints contain also lower and upper bounds on the parameters of the enveloping function which has not been considered in earlier studies. Making use of the expression for the PSD function $G(\omega)$ of Eq. (9), the optimization formulation in Eq. (17) can be rewritten as:

$$\begin{aligned}&\text{Minimize } \beta\\ &\text{Such that } \sum_{n=1}^{N_f}\sigma_n^2 = \overline{E}_0; \frac{1}{2\pi}\sqrt{\frac{\sum_{n=1}^{N_f}\omega_n^2\sigma_n^2}{\sum_{n=1}^{N_f}\sigma_n^2}} = \overline{n}_0^+;\\ &\frac{1}{2(\omega_c-\omega_0)}\sum_{n=1}^{N_f}(\omega_n-\omega_{n-1})\log_e[1+\frac{\sigma_n^2}{G_0(\omega_n-\omega_{n-1})}] \geq \Delta\overline{H}_W; \qquad (18)\\ &\alpha_{1l} \leq \alpha_1 \leq \alpha_{1u}; \alpha_{2l} \leq \alpha_2 \leq \alpha_{2u}; \alpha_2 > \alpha_1 > 0;\ \sigma_n^2 \geq 0; n = 1,2,...,N_f.\end{aligned}$$

The decision variables for this optimization problem are $\sigma_1^2, \sigma_2^2, ..., \sigma_{N_f}^2, \alpha_1, \alpha_2$. The solution to this constrained nonlinear optimization problem is solved using sequential quadratic programming (SQP) method as will be demonstrated in the numerical examples.

As mentioned in the Introduction section, earlier models of seismic critical earthquake

loads assume the availability of a set of past recorded ground motions which is used in quantifying the constraint bounds $\overline{E}_0, \overline{n}_0^+$ and $\Delta\overline{H}_{\mathrm{W}}$. However, it is easier and more reliable to find a response spectrum specified for a given location rather than complete information on past recorded earthquake accelerations. In fact, most seismic codes specify design response spectrum based on site soil conditions of the region. In the present study we assume that the knowledge on the seismicity of the site considered is limited to a smooth design response spectrum. In fact, the characteristics of earthquake ground accelerations are implicitly contained in the design response spectrum of the site [25,26]. We propose that the available design response spectrum be used in generating a set of ground accelerations that are used for quantifying the constraint limits that the future earthquake needs to satisfy. The subject of simulating earthquake accelerations compatible with a specified design response spectrum is well established in the literature. See, for example, references [27-29].

The given spectrum is used to generate compatible ground accelerations. In the simulation process the procedure proposed by Deodatis [29] is adopted. The simulation process starts by reading the data of the target design response spectrum (TDRS) and the modulating function $A(t)$. The non-stationary acceleration $\ddot{x}(t)$ to be simulated is expressed as a product of a stationary acceleration $\ddot{v}(t)$ and an envelope function $A(t)$. This representation is similar to the representation of the non-stationary random process $\ddot{u}_{\mathrm{g}}(t)$ of Eq. (5). In other words, we simulate samples of the random accelerations $\ddot{v}(t)$ and $\ddot{x}(t)$ Once the TDRS is defined, a sample of $\ddot{v}(t)$ is generated starting from the PSD function of a white noise random process of intensity G_0. Subsequently, a sample of the non-stationary acceleration $\ddot{x}(t)$ is computed by multiplying the sample of $\ddot{v}(t)$ by the modulating function $A(t)$. The response spectrum of the acceleration $\ddot{x}(t)$ is then computed for the same frequency range of the target design response spectrum. The PSD function of the stationary process $\ddot{v}(t)$ is updated by a frequency factor that equals the ratio of the spectrum of the TDRS and that of the ground acceleration $\ddot{x}(t)$ New samples of the ground accelerations $\ddot{v}(t)$ and $\ddot{x}(t)$ are then generated. The algorithm iteratively updates the PSD function of the stationary acceleration and a new sample of the non-stationary acceleration is produced. No explicit convergence criterion is enforced. A few iterations are seen to be adequate to produce a ground acceleration history that matches the given TDRS.

The quantification of the constraint limits $\overline{E}_0, \overline{n}_0^+$ and $\Delta\overline{H}_{\mathrm{W}}$ of Eq. (18) is performed based on numerical analysis of the set of simulated ground accelerograms. The constraint parameter $\overline{E}_0$ is taken as the maximum value across the set of simulated accelerations. The parameters $\overline{n}_0^+$ and $\Delta\overline{H}_{\mathrm{W}}$ are taken as the average quantities across the ensemble.

3. THE USE OF RESPONSE SURFACE METHOD AND FORM FOR THE RELIABILITY ANALYSIS

The performance function of Eq. (16) is implicitly defined in the space of $2N_{\mathrm{f}}$+1 random

variables denoted collectively by the vector $\mathbf{X} = [R, A_1, A_2, ..., A_{N_f}, B_1, B_2, ..., B_{N_f}]^t$. As mentioned in the previous section, the envelope parameters are treated as deterministic quantities. The first step in implementing the response surface method for reliability computation consists of transforming the basic random variables **X** into a vector of standard normal random variables denoted by **Y**. The response surface method pursued here replaces the implicit performance function in Eq. (16) by an approximate quadratic surface [24]:

$$\overline{g}(\mathbf{Y}) = a + \sum_{i=1}^{N_{rv}} b_i Y_i + c_i Y_i^2 \tag{19}$$

Here N_{rv}= 2 N_f +1 is the number of basic random variables on which the performance function depends and a, b_i, c_i, i = 1,2,…, N_{rv} are the unknown deterministic parameters to be determined. The form of the response surface adopted in the above equation does not consider the cross quadratic terms. The inclusion of these terms would lead to considerable increase in the computational effort although the framework of solution remains essentially the same. This aspect is examined later in the numerical examples. It must be noted also that the problem of determination of the reliability index β_{HL} constitutes a constrained nonlinear optimization problem [30]. This optimization problem, in turn, is embedded into the optimization problem associated with the determination of the critical earthquake load. Consequently, the algorithm proposed in the present study for computing the critical earthquake loads, consists of two optimization routines. The outer routine is meant for computing the critical excitations, and the inner routine, that computes β_{HL}, is called by the outer routine at each major step of computing the critical input. The steps involved in these calculations are:

(a) Outer optimization for estimating critical excitations

1. Use the site design response spectrum to simulate sample ground accelerations and quantify the constraint bounds $\overline{E}_0, \overline{n}_0^+$ and $\Delta\overline{H}_W$.
2. Select the failure criterion of the structure, define the distributions and distribution parameters of the basic random variables, and make initial guess for the optimization variables $\sigma_i^2, i = 1,2,.., N_f$.
3. Define the performance function $g(R, \sigma_1^2, \sigma_2^2, ..., \sigma_{N_f}^2)$ of Eq. (16).
4. Make an initial guess for the failure point $x_{i0}^*; i = 1,2,..., N_{rv}$ and compute the associated point $y_{i0}^*; i = 1,2,..., N_{rv}$ in the standard uncorrelated normal space. Here, the transformation $\mathbf{Y} = \mathbf{T}'\mathbf{X}'$ is used, where $X_i' = (X_i - \mu_i)/\sigma_i$ is the reduced variate and **T** is a transformation matrix. Details of this transformation are provided in [23].
5. Call the basic optimization routine that provides new values for the optimization variables $\sigma_i^2, i = 1,2,.., N_f$.

(b) Inner optimization for β_{HL} computation

1. Fit a response surface in the uncorrelated standard normal space. Thus, the actual implicit performance function is approximated with a closed form function at the failure point. In the present work, we use a quadratic polynomial function as given in Eq. (19). The steps of this fitting can be summarized as follows:

- Sample **Y** in Eq. (19) at $2N_{rv}$+1 points (at mean, μ_i, and mean $\pm f\overline{\sigma}_i$ of these random variables). Here, f is a constant and $\mu_i, \overline{\sigma}_i$ are mean and standard deviation of Y_i, respectively.
- Evaluate the actual performance function, $g(\mathbf{Y})$ at the $2N_{rv}$ +1 points. Here, the quantity $\max_{0<t<\infty} | z(x_0, t, \alpha_1, \alpha_2, A_i, B_i) |; i = 1,2,..., N_{\mathrm{f}}$ is computed using numerical integration of the governing equations of motion (Eq. 2).
- Solve the set of 2 N_{rv} +1 algebraic equations given by **A B** = **G**, to determine the constants a, b_i, c_i, $i=1, 2,\ldots, N_f$. Here **A** is a square matrix of size 2 N_{rv} + 1 and the matrices **B** and **G** are of the size 2 N_{rv}+1 by 1. The details of these matrices can be found in reference [19].
- Use the explicit limit surface $\overline{g}(\mathbf{Y})$ to calculate the reliability index, β_{HL} and the associated design point $y_i^*; i = 1,2,..., N_{rv}$. The procedures for these calculations are standard and the details of these computations are provided in [23]. This includes iterative calculation of the reliability index, evaluation of the performance function and updating the check-point. The algorithm is stopped when the convergence criteria $| \beta_{\mathrm{HL}_j} - \beta_{\mathrm{HL}_{j-1}} | \le \delta_1$ and $| g_j(\mathbf{Y}) | \le \delta_2$ are satisfied, where δ_1 and δ_2 are small quantities to be selected.
- Update the starting point $\overline{\mu}_i$ to $y\mu_i = \overline{\mu}_i + (y_i^* - \overline{\mu}_i) \dfrac{g(\overline{\mu}_i)}{g(\overline{\mu}_i) - g(y_i^*)}; i = 1,2,...,2N_{rv}+1$ and refit a new response surface using the new updated point.

2. Check convergence of the basic optimization routine $| g_j(\mathbf{Y}) | \le \delta_2, | \sigma_j^2 - \sigma_{j-1}^2 | \le \delta_3$. If convergence is achieved go to next step, otherwise go to step 4.
3. Store the quantities $\sigma_i^2, \beta_{\mathrm{HL}}, x_i^*, \alpha_i; i = 1,2,..., N_{rv}$.

The computation of reliability-based critical earthquake excitations, as developed above, provides different input-response descriptors. This includes critical PSD function that produces the least β_{HL} associated β_{HL} and notional failure probability, $P_{f_0} = \Phi(-\beta_{\mathrm{HL}}) = 1 - \Phi(\beta_{\mathrm{HL}})$. Here, Φ is the standard Gaussian probability distribution function. The formulation leads also to a critical time history at the design point, given as $\ddot{u}_{\mathrm{g}}(t) = e(t) \sum_{i=1}^{N_{\mathrm{f}}} A_i^* \cos \omega_i t + B_i^* \sin \omega_i t$. Here, A_i^*, B_i^* correspond to the point in the original space of random variables to which the failure point in the standard normal space gets mapped. Finally, the vector $\gamma_i; i = 1,2,..., N_{rv}$ provides a measure of sensitivity of reliability index with respect to individual random variables **X**.

Thus the steps in computing critical earthquake loads from response spectra for elastic

structures are: (1) quantifying the constraints from the site response spectrum (2) establishing the outer optimization for critical earthquake calculation and (3) the inner optimization for β_{HL} computation. The next section extends this approach to inelastic structures.

4. CRITICAL EARTHQUAKE EXCITATIONS FOR BILINEAR HYSTERETIC STRUCTURES

4.1 Dynamic analysis of bilinear hysteretic structures

The inclusion of inelastic structural behavior is of central importance in earthquake-resistance design. This is particularly true when dealing with extreme loads as is the case with seismic critical excitations. The response of inelastic structures has a non zero mean and is non-Gaussian even if the seismic input is Gaussian with zero mean. The equation of motion governing the relative displacement response $u(t)$ of a one-story structure modeled as a single-degree-of-freedom system subjected to a single component of earthquake acceleration $\ddot{u}_{\mathrm{g}}(t)$ at its base (see Figure 1(a)) is given by:

$$m\,\ddot{u}(t) + c\,\dot{u}(t) + f_s(t) = -m\,\ddot{u}_{\mathrm{g}}(t). \tag{20}$$

Here, m, c, are, respectively, the mass and damping of the SDOF, $f_s(t)$ is the inelastic restoring force in the spring. For linear SDOF systems this force is a linear function of the spring coefficient k and the displacement response $u(t)$ and for inelastic systems $f_s(t)$ is a nonlinear function of the displacement response $u(t)$. Figure 1(b) depicts the nature of $f_s(t)$ for hysteretic inelastic systems.

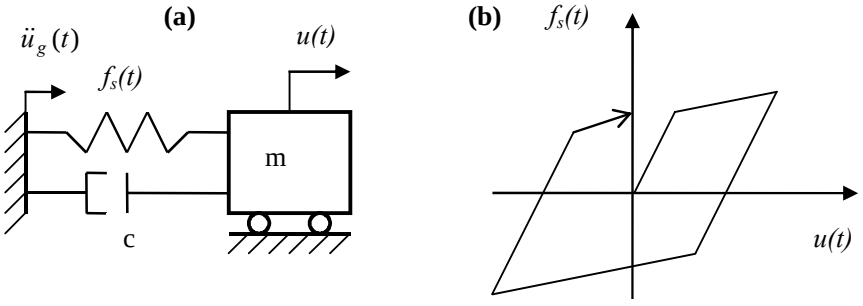

Figure 1. (a) bilinear hysteretic SDOF system (b) force-displacement relationship

For dynamic systems governed by the above equation of motion the force-deformation relation is no longer a single valued relation. Thus, for a displacement $u(t_i)$ at time t_i the resisting force depends upon prior history of motion of the system and whether velocity

response $\dot{u}(t_i)$ is increasing or decreasing. Assuming that damping is viscous and that the system starts from rest, the above equation reduces to:

$$\ddot{u}(t) + 2\varsigma\omega\,\dot{u}(t) + \omega^2 u_y \bar{f}_s(t) = -\ddot{u}_g(t), \tag{21}$$

where, ς is the damping ratio, ω is the natural frequency for the elastic system or for the inelastic system undergoing small deformations (i.e. $u < u_y$) and u_y is the yield displacement. The function $\bar{f}_s(t)$ may be viewed as the spring restoring force in a dimensionless form. Referring to Eq. (21) it may be noted that for a given earthquake acceleration $\ddot{u}_g(t)$, the inelastic displacement response depends on the natural frequency ω, the damping ratio ς and the yield displacement u_y (see Figure 1(b)). Herein, the yield displacement u_y is defined as f_y / k where f_y is the yield strength. The maximum inelastic displacement of the structure normalized to the yield displacement is known as the ductility factor and is an important parameter for design of inelastic structures. An incremental differential equation is obtained by expressing Eq. (21) at time t_i and $t_i + \Delta t$ [31]. The numerical integration to this equation is carried out using the Newmark-β method and more details are provided in reference [5]. The details of the computation of the reliability index using the response spectrum were provided in Section 2.3.

4.2 Energy dissipated by inelastic structures

To gain more insights into the nature of critical earthquake loads computed for inelastic structures, it is of interest to quantify various forms of energy dissipated by the inelastic system. Several authors employed the energy dissipated by the structure in characterizing response analysis of dynamical systems [32,33]. These energy terms can be quantified by integrating the structure equation of motion. Thus, the energy balance for the inelastic system can be written as (see Eq. (21)):

$$\int_0^u m\,\ddot{u}(t)\,du + \int_0^u c\,\dot{u}(t)\,du + \int_0^u f_s(t)\,du = -\int_0^u m\,\ddot{u}_g(t)\,du. \tag{22}$$

The right side of the above equation represents the input energy to the structure since ground starts shaking until it comes to rest. The first energy term of the left side is the kinetic energy $E_K(t)$ of the mass associated with its motion relative to the ground and is given as:

$$E_K(t) = \int_0^u m\,\ddot{u}(t)\,du = \int_0^{\dot{u}} m\,\ddot{u}(t)\,d\dot{u} = \frac{m[\dot{u}(t)]^2}{2}. \tag{23}$$

The second term of the left side of Eq. (22) represents the energy dissipated by viscous damping $E_D(t)$ given by:

$$E_{\mathrm{D}}(t) = \int_0^u c\,\dot{u}(t)\,du = \int_0^t c\,[\dot{u}(t)]^2\,dt. \tag{24}$$

The third term of Eq. (22) is the sum of the recoverable strain energy $E_S(t)$ and the energy dissipated by yielding $E_{\mathrm{Y}}(t)$ and are given as:

$$E_{\mathrm{S}}(t) = \frac{[f_s(t)]^2}{2k};\; E_{\mathrm{Y}}(t) = \int_0^u f_{\mathrm{s}}(t)du - E_{\mathrm{S}}(t) = \int_0^t \dot{u}(t) f_s(t)dt - E_{\mathrm{S}}(t). \tag{25}$$

The parameter *k* appearing in the above equation is the initial stiffness of the inelastic system. In the present study, the time-variation of energy terms given in Eqs. (23-25) are employed in quantifying and characterizing various forms of energy dissipated by the inelastic system.

The computation of reliability-based non-stationary critical earthquake loads (Sections 2, 3 and 4) involves the following: (1) Quantifying the constraints imposed on the earthquake load (outer optimization) from the site response spectrum (2) Using the response surface method to replace the implicit performance function with an explicit quadratic limit state (3) Establishing the inner optimization using FORM to evaluate the system reliability index, and (4) Establishing the outer optimization that optimizes the parameters of the earthquake load (PSD and envelope functions).

It may be noted that the framework for computing critical excitations for linear and hysteretic systems is essentially the same. The difference is in the algorithm adopted for the dynamic analysis which is embedded in the response surface fitting.

4.3 Inelastic MDOF structures

The formulation developed in Section 4.1 computes non-stationary random critical earthquake loads on inelastic SDOF structures. The algorithm presented for the dynamic analysis computes the seismic response for SDOF structures. The formulation of Section 4.1 can be extended to handle MDOF structures if the dynamic analysis tackles MDOF systems. This can be achieved by linking the methodology developed in the present paper with finite element software. The use of the finite element is to compute the structure's inelastic response which is needed in the inner optimization routine and the response surface fitting.

5. NUMERICAL EXAMPLES

To demonstrate the formulations developed in the preceding sections, three numerical examples are considered. The first two examples demonstrate the methodology for elastic single- and multi-story frame structures, respectively. The third example considers a structure with inelastic behavior.

5.1 Example 1: Single-story elastic frame structure

5.1.1 Structure considered

A single-story steel frame structure is considered. The frame structure has width L = 9.14 m, height h = 5.49 m and modulus of elasticity E = 210 Gpa. The columns are made of W 10×33 steel section and the girder supports a total dead load of 3×10^3 N/m. The stiffness of columns is computed to be 4.67×10^5N/m. For purpose of dynamic analysis it is assumed that the girder is rigid to prevent rotation and columns are massless. Accordingly, the frame structure is modeled as an SDOF system. The natural frequency of the frame structure was computed as $\omega_n = 2.07$ Hz and a modal viscous damping of 3 % is considered. The failure criterion of the frame structure is defined in terms of the spring force (shear force in columns). The structure is considered to fail if the force in the spring exceeds a threshold value R. Herein, R is taken as a normal random variable of mean $\mu_R = 2\times10^3$ N and standard deviation $\sigma_R = 200$ N.

5.1.2 Quantification of constraints from the site response spectrum

The quantification of the constraint limits imposed on the future design earthquake (Eq. 18) is based on numerical analysis of a set of 20 simulated earthquake accelerations compatible with the TDRS of the site. The TDRS adopted in this example is taken for a firm soil site [34,35], see Figure 2(a). The acceleration duration is taken as 20 sec.

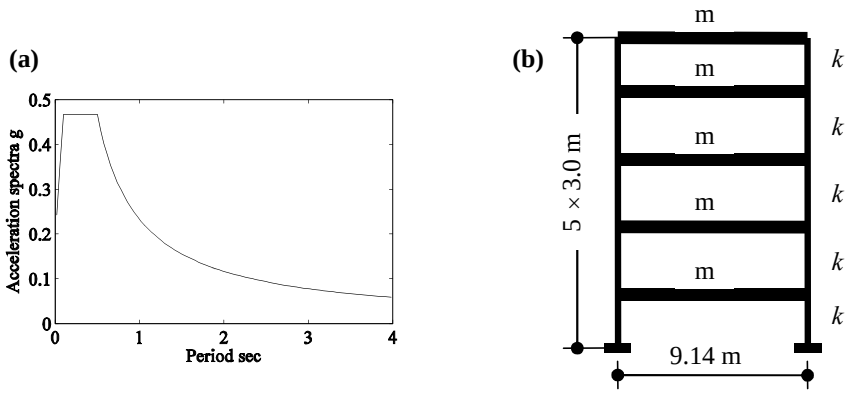

Figure 2. (a) design response spectrum (b) multi-story frame structure

Table 1: Statistics of simulated accelerations from the site response spectrum

Parameter	E_0 **(m²/s⁴)**	E_2 **(m²/s⁶)**	E_T **(m²/s⁴)**	n_0^+ **(Hz)**	$\Delta\overline{H}_W$
μ	1.37	296.11	20.17	2.25	0.1369
σ	0.16	31.93	3.21	0.11	0.0137

Table 1 summarizes the statistics of the parameters E_0, E_2, E_T, n_0^+ and $\Delta\overline{H}_W$ for the simulated acceleration. Herein, $\Delta\overline{H}_W$ is calculated with respect to a white noise random process of intensity = 0.02. It is observed that the variations in E_0 and E_2 are higher than variations in n_0^+ and $\Delta\overline{H}_W$. This observation is consistent with features usually observed in actual recorded ground motions. The average value of $\overline{n}_0^+ = 2.25$ is significantly matching with the dominant frequency of 2.50 Hz for a random process described by the Kanai-Tajimi PSD function for a stiff soil site [36].

In the numerical calculations, the constraint quantity $\overline{E}_0$ is taken as the peak value across the ensemble (1.47 m^2/s^4) and the quantities $\overline{n}_0^+$ and $\Delta\overline{H}_W$ are taken as the average values given in Table 1. The lower and upper limits on the envelope parameters are taken as $\alpha_{1l} = 0.10, \alpha_{2l} = 0.35$ and $\alpha_{1u} = 0.25, \alpha_{2u} = 0.50$. Figure 3(a) depicts a sample ground acceleration of the generated 20 time histories. It was observed that the convergence of the iterative scheme employed for generating ground accelerations compatible with TDRS is achieved within a number of iterations of about 10. For instance, the response spectrum of the simulated acceleration shown in Figures 3(b) is obtained with 7 iterations. Figure 4 shows the Fourier spectrum of the simulated acceleration and also for an actual ground acceleration recorded at a firm soil site. Both plots indicate a frequency content of 0-10 Hz and a dominant frequency of about 2.0 Hz. Critical earthquake loads are computed using sequential quadratic optimization method through the Matlab Optimization Toolbox [37] using the '*fmincon'* algorithm. The convergence limits of the optimizations are taken as $\delta_1 = 10^{-3}, \delta_2 = 10^{-6}$ and $\delta_3 = 10^{-6}$. It may be emphasized that it is difficult to prove that the optimization will converge to the global optima. However, the optimal solution was verified by starting the optimization with alternative initial guesses. While implementing this procedure, several alternative starting solutions from within the feasible region were considered and it was observed that all the starting solutions lead to the same maximum. The solution was also verified with the qualitative feature expected for the ground acceleration, dynamic response of the structure and constraints imposed.

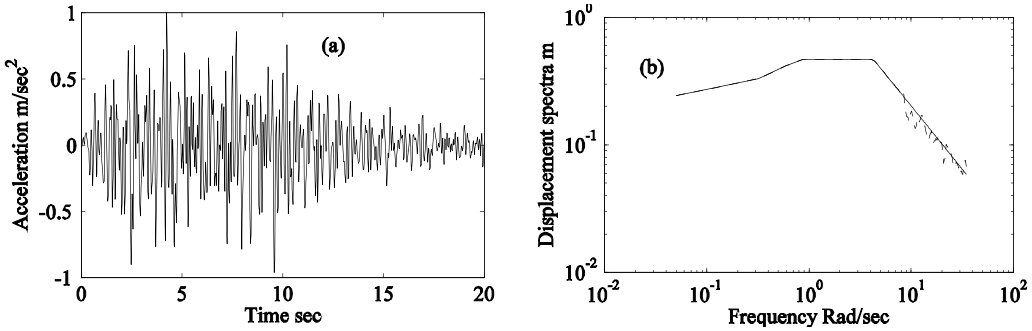

Figure 3. Simulated acceleration compatible with target response spectrum (a) time history (b) response spectra (—— target spectra, — — simulated acceleration)

In the numerical calculations, the frequency range of the ground acceleration (ω_0, ω_c) is taken as (0,10) Hz which is expected to cover well the frequency range of an earthquake signal at a stiff site. The number of frequency terms retained in the series representation (Eq. (7)) is taken as N_f = 101 which implies that the performance function is defined in a space of 203 random variables. This number was selected based on a study of the sensitivity of the reliability index with respect to the number of frequencies retained N_f. The frequencies $\omega_i, i = 1,2,..,N_f$ are distributed such that one of these frequencies coincides exactly with the structure natural frequency ω_n and more frequencies are placed within the bandwidth of ω_n. Two cases of constraints are considered. In the first case constraints on total average energy and zero-crossing rate are considered and in the second case these two constraints as well as the entropy rate constraint are considered.

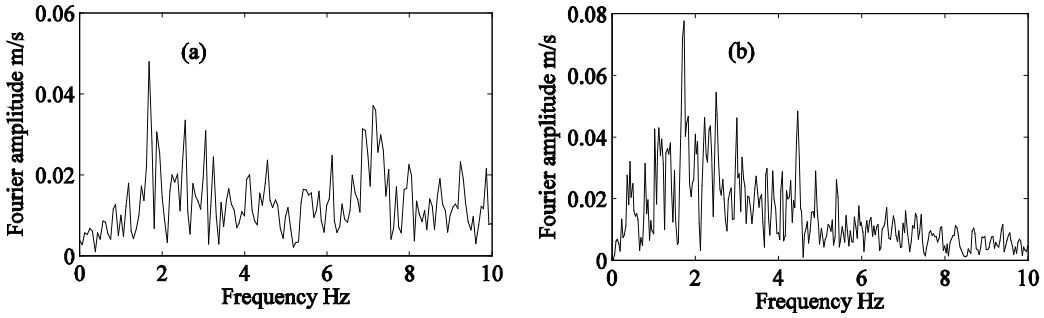

Figure 4. Fourier spectrum (a) simulated ground acceleration (b) 1989 Loma Prieta earthquake (W-component)

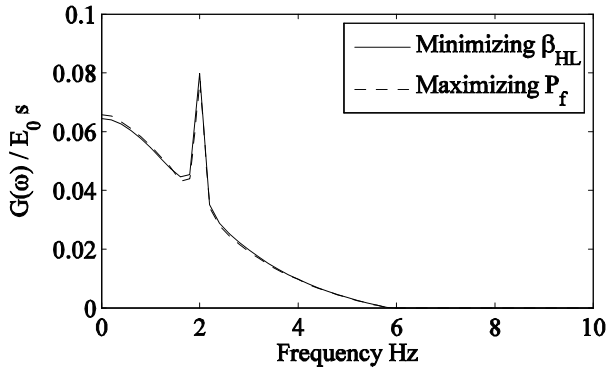

Figure 5. Example 1: verification of response surface method, case 2 (—— maximizing β_{HL}, — — maximizing P_f)

5.1.3 Results and discussions

The calculation of β_{HL} in this paper is based on the use of response surface modeling. For the method to be successful it is required that: (a) The failure surface in the transformed standard

normal space does not possess more than one region which makes comparable contributions to the failure probability, and (b) The response surface provides an acceptable fit to the failure surface near the failure point. For the problem on hand, it is difficult to prove that these conditions are invariably met for all choices of the parameters of the problem. However, for specific cases limited verifications are possible. To illustrate this, we consider the case when the ground acceleration is modeled as a stationary Gaussian process and the structure is taken to be linear. In this case the response process is Gaussian and the extreme of this process over a specified time duration can be approximated by a Gumbel random variable. This would mean that the probability of failure of the structure with respect to the performance function as in Eq. (16) can be determined without taking recourse to response surface modeling. This in turn, means that the critical PSD function here can be determined directly by maximizing the failure probability without adopting the response surface approach. The exact results on the critical PSD function so obtained is compared in Figure 5 with corresponding results based on response surface based procedure. The two results show nearly the same behavior. This, at least to a limited extent, verifies the applicability of the response surface approach to the present problem. For the general case when the structural inelastic behavior and nonstationary of the ground acceleration are considered, this type of verification is difficult to make. In the present study, we proceed with the promise that the results for this general case can be considered acceptable if the results obtained are qualitatively consistent with the known features of the dynamic response of inelastic structures, constraints imposed and critical PSD function obtained.

Figure 6 shows the PSD function of the critical acceleration $\ddot{w}_{\mathrm{g}}(t)$ for cases 1 and 2, respectively. The associated critical envelope function $e(t)$ (see Eq. 6) and a sample critical acceleration $\ddot{u}_{\mathrm{g}}(t)$ are shown in Figure 7 for case 2. The reliability index of the structure is computed to be -1.88 and 2.87 for cases 1 and 2, respectively. The associated notional failure probabilities are computed to be 9.87×10^{-1} and 2.05×10^{-3}, respectively. Similarly, the peak value of the displacement response standard deviation (Eq. 10) reduces from 0.0972 m to 0.0395 m when the entropy rate constraint is brought in. It is also seen that for case 1, the PSD function has dominant amplitude at the structure natural frequency with low amplitudes on either side of the structure natural frequency. The low amplitude at frequencies other than the structure frequency ensure the satisfaction of the constraint imposed on the zero-crossing rate.

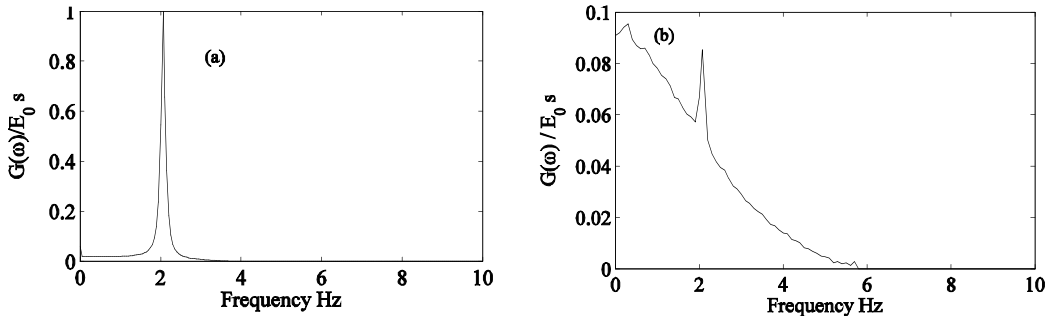

Figure 6. Example 1: power spectral density function for $\ddot{w}_g(t)$ (a) case 1 (b) case 2

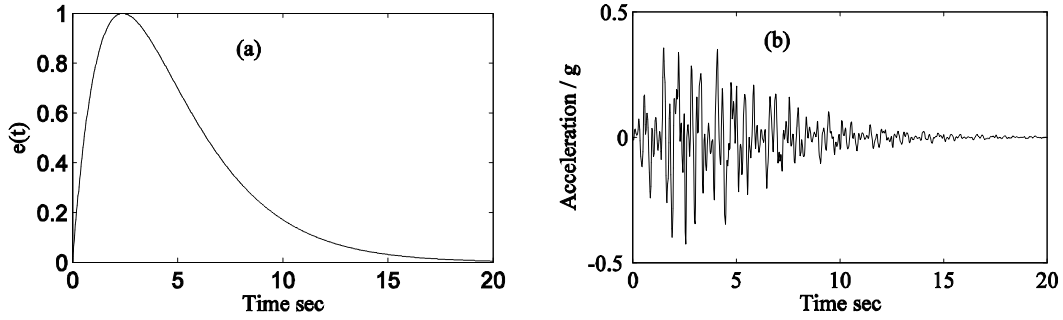

Figure 7. Example 1, case 2: (a) critical envelope (b) sample critical acceleration $\ddot{u}_g(t)$

The inclusion of the entropy rate leads to the redistribution of the power of the PSD function across wider range of frequencies compared to case 1 (see Figure 6(b)). In other words, the entropy rate constraint leads to a wide band earthquake signal with the associated PSD function having its geometric center being shifted from the structure fundamental frequency. Relatively small peak amplitude, however, is yet observed at the structure natural frequency. This is also evident from the increase of the reliability index from -1.88 for case 1 to 2.87 for case 2. The result of case 2 is seen to be realistic in terms of the shape of the PSD function and response produced. Case 1, on the other hand, does not lead to a realistic description of real earthquake load. This is because the amplitude of recorded ground motions is always characterized by the nonlinear soil amplifications at the site. To compare numerical results from critical earthquake loads with those obtained from existing earthquake models, we compute the reliability index when the structure is subjected to Kanai-Tajimi PSD function valid for a stiff soil site. The reliability index obtained from Kanai-Tajimi model of central frequency 2.0 Hz [35] was 3.97 which reveals a factor of about 1.40 compared to the associated value computed from critical input of case 2. Therefore, critical earthquake models produce relatively conservative responses.

5.2 Example 2: Multi-story elastic frame structure

To demonstrate the applicability of the formulation developed in the present paper to MDOF structures, we consider the five-story reinforced concrete shear frame of Figure 2(b). The structure has a span width of 9.14 m and floors height of 3.00 m, modulus of elasticity $E = 2.0\times10^{10}$ N/m^2 and columns have square cross-sections of 0.30 m. The stiffness of columns in each floor is computed as $k = 6\times10^6$ N/m and girders carry a dead load of 3.00 KN/m. The free vibration analysis showed that the first five natural frequencies are 0.68, 1.97, 3.11, 3.99 and 4.55 Hz, respectively. A modal viscous damping of 5 % damping ratio is considered for all the modes and dynamic analysis is carried out by retaining contribution from the five modes. The performance function of Eq. (16) is defined in terms of the displacement response of the top floor. The resistance R is taken as a deterministic quantity R=0.04 H=0.04×15=0.6m. The same constraint quantities and convergence limits adopted in Example 1 are used in this example.

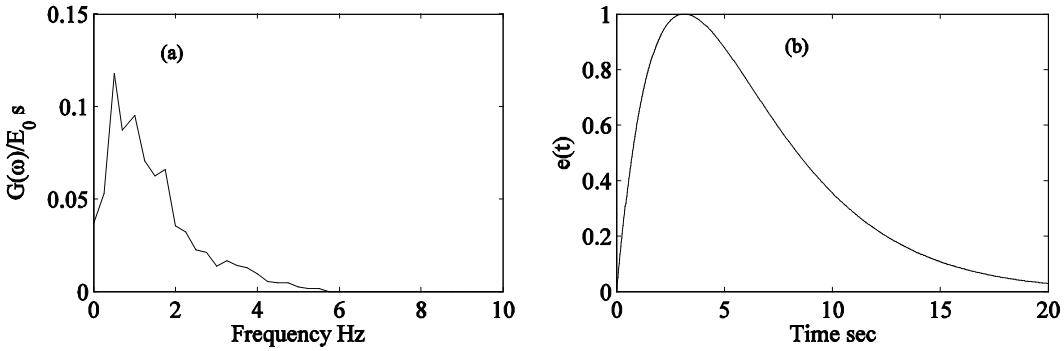

Figure 8. Example 2, case 2: (a) critical PSD function for $\ddot{w}_g(t)$ (b) critical envelope

The PSD function of the stationary acceleration, for case 2, is shown in Figure 8(a) and the associated envelope function is presented in Figure 8(b). Figures 9(a) and 9(b) show a sample of the critical acceleration and the sensitivity variables, respectively.

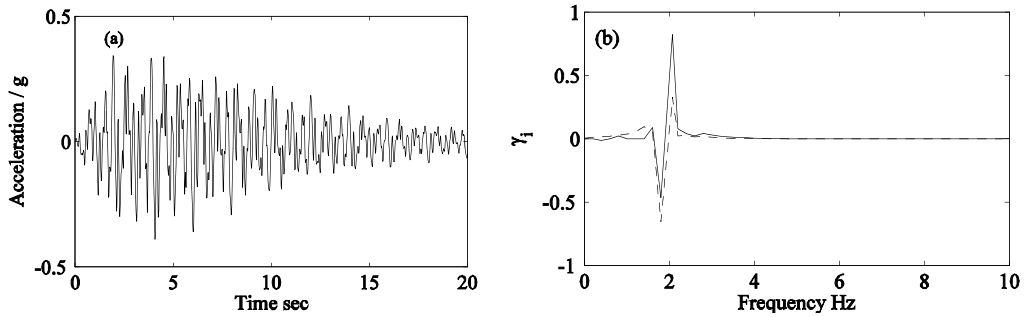

Figure 9. Example 2, case 2: (a) sample acceleration $\ddot{u}_g(t)$ (b) sensitivity indices —— A_i,— — B_i

In general, the feature observed in Example 1 is also observed in the present example. The frequency range of the PSD function is similar to that of example 1. This in turn implies that the frequency range of the ground acceleration depends on the soil profile and not on the structure properties. Furthermore, it is observed that the PSD function has a peak at the fundamental natural frequency of the structure. However, this peak is not high as was the case with the single-story frame structure of Example 1. A minor peak is also observed at a frequency close to the second natural frequency of the structure. The reliability index obtained for constraints scenarios 1 and 2 were -1.49 and 1.70, respectively. The sensitivity analysis of the reliability index with respect to 1 % changes in the constraint parameters $\overline{E}_0, \overline{n}_0^+$ and $\Delta\overline{H}_W$ revealed that the percentage changes in reliability index are 1.47 %, 0.48 % and 1.79 %, respectively. It was also observed that the reliability index is sensitive to the random variables corresponding to the structure first two natural frequencies.

5.3 Example 3: Single-story inelastic frame structure

We reconsider the same steel frame structure of Example 1 with the important difference that the inelastic behavior of the structure is considered. The force-displacement relation is taken to be elastic-plastic. The initial stiffness of the columns is taken as 4.67×10^5 N/m and the natural frequency of the inelastic structure undergoing small deformation is $\omega_n = 2.07$ Hz. A modal viscous damping of 3 % is considered. The yield strength of the spring force in tension and compression is taken as 2×10^4 and -2×10^4 N, respectively. This, in turn, implies that the yield displacements in tension and compression are 0.0428 and -0.0428 m, respectively. The same constraint quantities and convergence limits of Example 1 are adopted.

The results of this example are shown in Figures 10 to 14. Figure 10 shows the convergence of the objective function β_{HL} in terms of the iteration number. In general, it is observed that the broad feature of critical PSD functions for alternative constraint scenarios resemble the features that have been observed for the elastic structure. We focus our attention, however, on the influence of the inclusion of the structure inelastic behavior on the critical seismic loads obtained. The following observations are made:

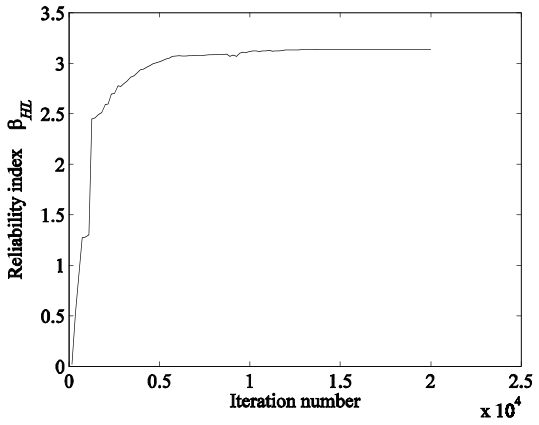

Figure 10. Example 3, case 2: convergence of objective function

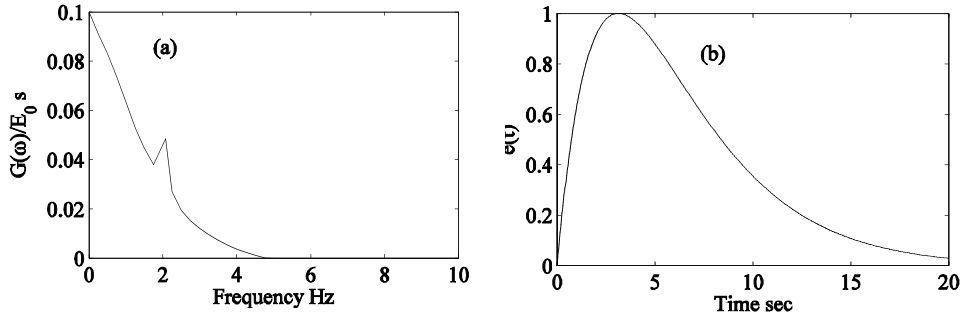

Figure 11. Example 3, case 2: (a) critical PSD function for $\ddot{w}_{\mathrm{g}}(t)$ (b) critical envelope

1. The results of constraints scenarios of cases 1 and 2 indicate the emergence of a peak at the elastic structure natural frequency. Such peak, however, is relatively smaller than the case of elastic structure (see, for example Figures 6(b) and 11(a)). It is seen also that entropy rate constraint is crucial in producing realistic earthquake input with the PSD function being broad band compared to case 1. For case 2, the reliability index β_{HL} was seen to increase from −1.32 to 3.16 as the entropy rate is brought in and similarly the ductility factor μ decreases from 3.4 to 2.15. A similar observation can also be made on the sensitivity indices where the plots of these factors display remarkable fluctuations near the natural frequency of the elastic structure.
2. The input acceleration at the design point for the elastic structure is narrow band with most energy lumped at the structure natural frequency ω (Figure 12(b)). The acceleration for the inelastic structure possesses amplitudes at a wider frequency range (0-5 Hz) (Figure 12(a)). A peak amplitude, however, exists close to ω. This is consistent with the feature observed in the PSD function. The inelastic displacement response has non zero mean (Figure 13) and permanent deformation is also observed.

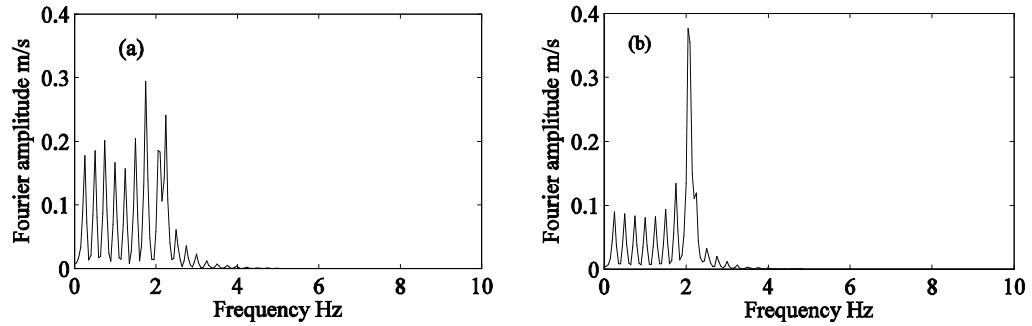

Figure 12. Example 3, case 2: critical acceleration $\ddot{u}_{\mathrm{g}}(t)$ at the design point (a) inelastic structure (b) elastic structure

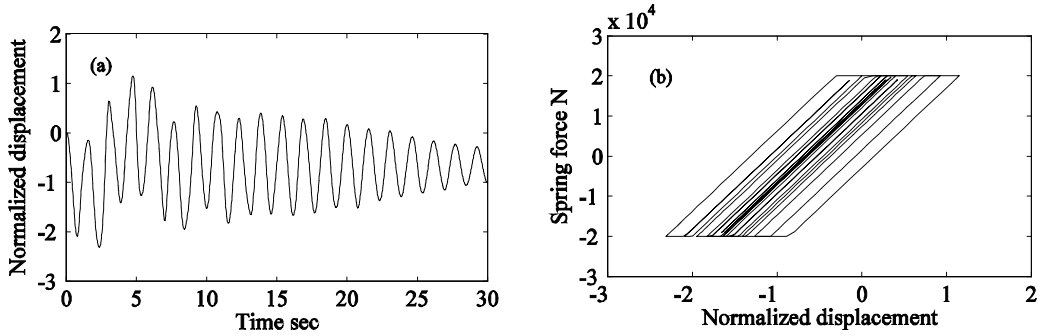

Figure 13. Example 3, case 2: (a) critical normalized response (b) restoring force-displacement hysteretic loops

3. The computation of the sensitivity indices indicates that these indices are higher at frequencies that are close to the structure fundamental frequency. This, in turn, implies that the reliability index is more sensitive to the random variables (A_i, B_i) that are close to the natural frequency of the elastic structure.
4. The input energy to the inelastic system from the critical acceleration $\ddot{u}_g(t)$ is primarily dissipated by yielding and damping of the structure (see Figure 14(a)). Unlike the elastic system, the kinetic and recoverable strain energy for the inelastic system are small and diminish near the end of the ground shaking (Figure 14(b)). The energy dissipated by yielding is significantly higher than that dissipated by damping. Viscous damping dissipates less energy from the inelastic system compared to that for the elastic system. This is because the velocity response is higher for the elastic system. It is also obvious that input energy to the inelastic system differs from the energy input to the elastic system.

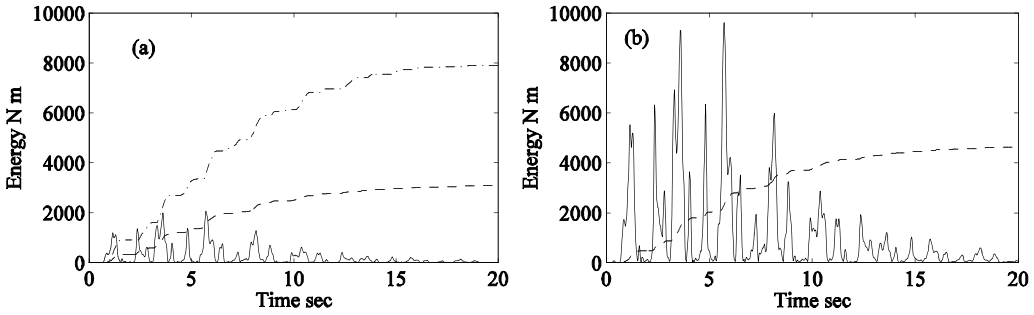

Figure 14. Example 3, case 2: dissipated energy under a sample critical acceleration $\ddot{u}_g(t)$ (a) inelastic structure —— E_K+E_S,— — E_D, — · — E_Y (b) elastic structure —— E_K+E_S,— — E_D

The form of the response surface assumed in Eq. (16) does not take into account the cross terms X_iX_j. The inclusion of these terms would lead to considerable increase in the computational effort although the framework of solution remains the same. To investigate the influence of including cross terms in the response surface model on the critical response and PSD functions, limited studies were conducted. The reliability index for cases 1 and 2, with the cross terms included, were computed to be −1.36 and 3.14, respectively. These results are marginally different from the corresponding results when the cross terms were excluded, which have already been computed to be −1.32 and 3.16 respectively. Similarly, the changes in critical power spectral density functions were also found to be marginally small. In this context it is to be noted that the fit for the response surface here is obtained in the space of standard normal random variables after the basic random variables, which are, in general, mutually dependent and non-Gaussian, have been transformed into mutually uncorrelated N(0,1) random variables. This would mean that the mutual dependencies in the basic random variables are implicitly taken into account in deriving the response surface even when cross terms in the model are not included. This possibly explains the marginal

influence that the cross terms in response surface model have on the final outcome of the case studies conducted.

6. CONCLUDING REMARKS

This paper develops a reliability-based computational methodology for non-stationary critical earthquake loads on elastic and inelastic structures. The new contributions developed in this paper include (1) developing a reliability-based non-stationary random critical earthquake loads from response spectra using the response surface method (2) accounting for uncertainty in the PSD function and the envelope function by treating these functions as unknowns (3) developing a general framework for handling structural hysteretic inelastic behavior (4) quantifying different forms of energy dissipated by the elastic and inelastic structures.

In the evaluation of the structural reliability in this study, the constraints on the critical earthquake input, such as, average zero crossing rate and entropy rate, have been treated as being deterministic in nature. One could treat these quantities also as random variables so that the uncertainties involved in their specification could be quantified. The probability distribution of these variables needs to be obtained based on studies such as the site specific uniform hazard analysis and study of local soil conditions. When these uncertainties are included one could derive the critical excitation model by optimizing the failure probability conditioned on these random variables and deduce the critical excitation models by using the theorems on conditional expectations. It is possible to model critical earthquake excitations based on uniform hazard spectra at a site but the constraints parameters should be treated as being random.

In general, critical earthquake loads were characterized by the constraints considered, site soil conditions and behavior of the structure (elastic or inelastic). The formulation developed leads to several descriptors of the input, such as, critical PSD function, critical reliability index and associated notional failure probability, sensitivity indices and a time history of the acceleration at the design point. It is shown that critical earthquake inputs for the inelastic structure differ from those for the elastic structure in terms of the above descriptors and also in terms of alternative energy forms dissipated by the structure. The input energy to inelastic structures is shown to be dissipated mainly by yielding and damping.

In the present study, the non-stationary ground acceleration was modeled as a uniformly modulated random process that is obtained by multiplying an envelope function and a stationary random process. This implies that the PSD function of the input acceleration does not depend on time. In this context, it is of interest to explore non uniform ground acceleration models using evolutionary PSD functions. It is possible to model the ground acceleration as being non-stationary in frequencies also which would add more complexity to the problem. This can be accounted for by using an envelope function that is a function of time and frequency as well. In this case, the formulation of the problem remains the same but the optimization problem needs to maximize the frequency parameters as well. It is also of interest to implement the formulation developed to complex MDOF inelastic structures. This can be achieved by using finite element method-based inelastic structural dynamic

analysis combined with the formulation proposed in this paper. Different models of inelasticity can also be studied.

Acknowledgement: This study is partly supported by funds from the U. S. Air Force Research Laboratory through subcontract to General Dynamics Information Technology (Contract No. USAF-0060-43-0001, Project Monitor: Mark Derriso). The support is gratefully acknowledged.

REFERENCES

1. Takewaki I. Seismic critical excitation method for robust design: A review, *Journal of Structural Engineering,* **128**(2002) 665-72.
2. Takewaki I. A Comprehensive review of seismic critical excitation methods for robust design, *Advances in Structural Engineering,* **9**(2006) 361-75.
3. Abbas AM, Manohar CS. Investigations into critical earthquake load models within deterministic and probabilistic frameworks, *Earthquake Engineering and Structural Dynamics,* **31**(2002) 813-31.
4. Abbas AM. Deterministic/reliability-based critical earthquake load models for linear/nonlinear engineering structures, Ph D thesis, Department of Civil Engineering, Indian Institute of Science, 2002.
5. Abbas AM. Critical seismic load inputs for simple inelastic structures, *Journal of Sound and Vibration,* **296**(2006) 949-67.
6. Drenick RF. Model-free design of aseismic structures, *Journal of Engineering Mechanics,* **96**(1970) 483-93.
7. Shinozuka M. Maximum structural response to seismic excitations, *Journal of Engineering Mechanics,* **96**(1970) 729-38.
8. Iyengar RN. Matched inputs. Report 47, Series J., Center of Applied Stochastics, Purdue University, West Lafayette, IN, 1970.
9. Drenick RF. Aseismic design by way of critical excitation, *Journal of Engineering Mechanics,* **99**(1973) 649-67.
10. Iyengar RN, Manohar CS. Nonstationary random critical excitations, *Journal of Engineering Mechanics,* **133**(1987) 529-41.
11. Iyengar RN. Critical seismic excitation for structures, *Proceedings of 5th ICOSSAR conference*, San Francisco, 1989, pp. 29-37.
12. Manohar CS, Sarkar A. Critical earthquake input power spectral density function models for engineering structures, *Earthquake Engineering and Structural Dynamics,* **24**(1995) 1549-66.
13. Takewaki I. Nonstationary random critical excitation for acceleration response, *Journal of Engineering Mechanics,* **127**(2001) 544-56.
14. Takewaki I. Probabilistic critical excitation for MDOF elastic-plastic structures on compliant ground, *Earthquake Engineering and Structural Dynamics,* **30**(2001) 1345-60.
15. Sarkar A. Linear stochastic dynamical system under uncertain load: inverse reliability analysis, *Journal of Engineering Mechanics,* **129**(2003) 665-71.

16. Saikat S, Manohar CS. Inverse reliability based structural design for system dependent critical earthquake loads, *Probabilistic Engineering Mechanics,* **20**(2005) 19-31.
17. Abbas AM, Manohar CS. Reliability-based critical earthquake load models. Part 1: Linear structures, *Journal of Sound and Vibration,* **287**(2005) 865-82.
18. Abbas AM, Manohar CS. Reliability-based critical earthquake load models. Part 2: Nonlinear structures, *Journal of Sound and Vibration*, **287**(2005) 883-900.
19. Abbas AM, Manohar CS. Reliability-based vector nonstationary random critical earthquake excitations for parametrically excited systems, *Structural Safety*, **29**(2007) 32-48.
20. Populis A. Probability, random variables and stochastic processes, McGraw-Hill, New York, 1991.
21. Kapur JN. Maximum entropy models in science and engineering. New Delhi, Wiley Eastern, 1993.
22. Moustafa A. Discussion of a new approach of selecting real input ground motions for seismic design: The most unfavourable real seismic design ground motions, *Earthquake. Engineering Structural Dynamics,***38**(2009) 1143-9.
23. Haldar A, Mahadevan S. Probability, Reliability and Statistical Methods in Engineering Design, John Wiley and Sons, Inc., NY, 2000.
24. Bucher CG, Bourgund U. A fast and efficient response surface approach for structural reliability problem, *Structural Safety,* **7**(1990) 57-66.
25. Vanmarcke EH, Gasparini DA. Simulated earthquake ground motion. *Proc. 4th Conf. on Structural Mechanics in Reactor Technology*, San Francisco, paper K1/9, 1973.
26. Preumont A. On the connection between the response spectrum and the spectral properties of earthquake accelerograms. *Proc., 4th Int. Conference on Applied Statistics and Probabilities in Soil and Structural Engineering*, Florence, 1983, 13-17 June.
27. Iyengar RN, Rao PN. Generation of spectrum compatible accelerograms, *Earthquake Engineering and Structural Dynamics,* **7**(1979) 253-63.
28. Preumont A. The generation of spectrum compatible accelerograms for the design of nuclear power plants, *Earthquake Engineering and Structural Dynamics,* **12**(1984) 481-97.
29. Deodatis G. Non-stationary vector processes: seismic ground motion applications, *Probabilistic Engineering Mechanics,* **11**(1996) 149-68.
30. Hasofer AM, Lind N. An exact and invariant first-order reliability format, *Journal of Engineering Mechanics,* **100**(1974) 111-21.
31. Paz M. *Structural dynamics*, Van Nostrand Reinhold Company, 2nd edition, NY, 1985.
32. Uang CM, Bereto VV. Evaluation of seismic energy in structures, *Earthquake Engineering and Structural Dynamics,* **19**(1990) 77-90.
33. Zahrah TF, Hall WJ. Earthquake energy absorption in SDOF structures, *Journal of Structural Engineering,* **110**(1984) 1757-72.
34. IBC. International *building code*, International code council Inc., USA, 2003.
35. ASCE. Minimum design loads for buildings and other structures, revision of ASCE-98, ASCE, Structural Engineering Institute, 2003.
36. Clough RH, Penzien J. *Dynamics of Structures*, McGraw-Hill, 2nd edition Tokyo, 1993.
37. Caleman T, Branch MA, Grace A. Optimization toolbox for the use with Matlab, user's guide version 2(Release 11), The Math Works Inc., USA, 1999.